Numerical Simulation and Analysis of Enzyme-Catalysed Substrate Conversion in a Microbioreactor

Linas Petkevičius and Romas Baronas

Faculty of Mathematics and Informatics,
Vilnius University, Naugarduko st. 24, Vilnius, Lithuania
Email: {linas.petkevicius, romas.baronas}@mif.vu.lt

***Abstract*—The paper presents a non-linear mathematical model for digital simulation of an enzyme loaded porous microreactor. The model is based on a system of reaction-diffusion equations, containing a non-linear term related to the Michaelis-Menten kinetics, and involves three regions: the enzyme microreactor where the enzyme reaction as well as mass transport by diffusion take place, a diffusion limiting region (the Nernst layer), where only the mass transport by diffusion takes place, and a convective region, where the analyte concentration is maintained constant. Assuming well stirred conditions, the influence of the thickness of the Nernst layer on the behaviour of the product emission, as well as the impact of the diffusion modulus and the Biot number has been numerically investigated. The simulation results showed that the Nernst layer must be taken into consideration when modelling micro-size bioreactors. The digital simulation was carried out using the finite difference technique.**

***Keywords*—reaction-diffusion; Michaelis - Menten kinetics; microbioreactor; CSTR.**

I. Introduction

Continuous-flow stirred tank reactors (CSTR) are common in chemical industries [1][2]. Although a stirred tank is a usual construction of industrial enzyme reactors, the effectiveness and optimal construction of CSTR remain open to study [3][4]. Specifically, further research is needed due to the application of the immobilized enzymes, such as biocatalysts, on a manufactoring scale that requires to use the reactors of different types, including CSTR [5][6][7].

A CSTR often refers to a model used to estimate the operation parameters when using a continuous agitated-tank reactor to reach a specified output [6]. In the last few decades, immobilized enzyme reactor models have evolved significantly with wide range of applications in food industry [8], waste cleaning [9], bacteria cells immobilization [10][11]. Rapid progress was noticed in integrating microfluidic reactors and biocatalytic reactions [12]. The combination of miniaturized technologies and microfluidics allows to increase the bioprocess efficiency. However, coupling microreactors and biocatalysis is highly complex, requiring an integrated approach addressing biocatalyst features, reaction kinetics, mass transfer and microreactors geometry [12][13].

Mathematical models have been widely used to investigate the kinetic peculiarities of the enzyme microreactors [7][12]. Models coupling the enzyme-catalysed reaction with the diffusion in enzyme microreactors are usually used. Since containing catalytic particles, the analyte in CSTR is well stirred and set in powerful motion, the mass transport by diffusion outside the microreactors is usually neglected [13][14]. In practice, the zero thickness of the diffusion shell (layer) can not be achieved [15]. We consider an array of identical spherical microreactors placed in a CSTR shown in Figure 1 [6], where area Ω_m denotes a microreactor, Ω_d denotes surrounding diffusion shell and Ω_c is a convective region.

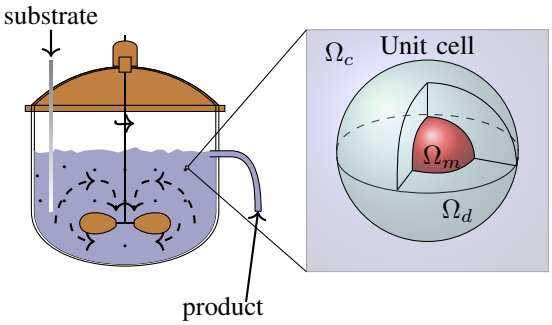

Figure 1. Continuous stirred tank reactor with enzyme-loaded microreactors (pellets) and a zoomed unit cell to be modelled.

The goal of this work was to investigate the dependencies of the internal and external diffusion limitations on the yield of the reaction product, modelled by reaction-diffusion equations, containing a non-linear term related to Michaelis-Menten kinetics [6][7][16]. The model involves three regions: the enzyme microreactor, where the enzyme reaction, as well as the mass transport by diffusion take place, a diffusion limiting region, where only the mass transport by diffusion takes place, and a convective region, where the analyte concentration is maintained constant. Due to a strong non-linearity of the reaction term, the computer simulation was carried out using the finite difference technique. [17].

The rest of the paper is organised as follows: in Section II, the mathematical model and microbioreactor characteristics are described; Section III formulates a dimensionless model and derives the main parameters of the bioreactor; Section IV describes the numerical model and the simulator; in Section V, results of numerical experiments are presented, and conclusions close the article.

 ISBN: 978-1-61208-594-4

II. Mathematical model

We consider an array of identical spherical microreactors placed in a continuous ideally stirred-tank reactor [6]. Assuming a uniform distribution of the microreactors in the tank and a relatively great distance between adjacent microreactors, the spherical unit cell was modelled by an enzyme-loaded microreactor (pellet) and a surrounding diffusion shell (the Nernst diffusion layer). The principal structure of the tank containing uniformly distributed microreactors and a unit cell are presented in Figure 1, where Ω_m denotes a microreactor (MR), Ω_d stands for the diffusion shell and Ω_c is a convective region.

In the enzyme-loaded MR layer we consider the enzyme-catalyzed reaction

$$\mathrm{E} + \mathrm{S} \underset{k_r}{\overset{k_f}{\rightleftharpoons}} \mathrm{ES} \xrightarrow{k_{\mathrm{cat}}} \mathrm{E} + \mathrm{P}, \tag{1}$$

where the substrate (S) combines reversibly with an enzyme (E) to form a complex (ES). The complex then dissociates into the product (P) and the enzyme is regenerated [18][19].

Assuming the steady-state approximation, the concentration of the intermediate complex (ES) does not change and may be neglected when modelling the biochemical behaviour of the microreactor [6][19][20]. In the resulting scheme, the substrate (S) is enzymatically converted to the product (P),

$$\mathrm{S} \xrightarrow{\mathrm{E}} \mathrm{P}. \tag{2}$$

A. Governing Equations

Assuming the symmetrical geometry of the microreactor and homogenised distribution of the immobilized enzyme inside the porous microreactor, the mathematical model can be described in one-dimensional domain using the radial distance.

Coupling enzymatic reaction in the microreactor (region Ω_m) with the one-dimensional-in-space diffusion, described by Fick's second law, and assuming the steady-state for a system (2) lead to the following governing equations of the reaction-diffusion type ($0 < r < R_0$):

$$D_{S,m}\frac{1}{r^2}\frac{\partial}{\partial r}\left(r^2\frac{\partial S_m}{\partial r}\right) = \frac{V_{\max}S_m}{K_M + S_m}, \tag{3a}$$

$$D_{P,m}\frac{1}{r^2}\frac{\partial}{\partial r}\left(r^2\frac{\partial P_m}{\partial r}\right) = -\frac{V_{\max}S_m}{K_M + S_m}, \tag{3b}$$

where r stands for space, $S_m = S_m(r)$ and $P_m = P_m(r)$ are the concentrations of the substrate and the reaction product in the microreactor, respectively, R_0 is the radius of the microreactor, $D_{S,m}$ and $D_{P,m}$ are the diffusion coefficients, $V_{\max} = k_{cat}E_0$ is the maximal enzymatic rate and $K_M = (k_r + k_{cat})/k_f$ is the Michaelis constant (see Figure 2(a)).

In the Nernst diffusion layer Ω_d only the mass transport by diffusion takes place:

$$D_{S,d}\frac{1}{r^2}\frac{\partial}{\partial r}\left(r^2\frac{\partial S_d}{\partial r}\right) = 0, \tag{4a}$$

$$D_{P,d}\frac{1}{r^2}\frac{\partial}{\partial r}\left(r^2\frac{\partial P_d}{\partial r}\right) = 0, \quad r \in (R_0,\ R_1), \tag{4b}$$

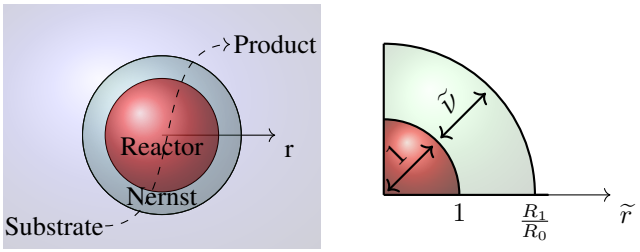

Figure 2. Principal structure of the unit cell consisting of a microbioreactor and the Nernst diffusion shell (a) and non-dimensionalized regions (b).

where $S_d = S_d(r)$ and $P_d = P_d(r)$ are the concentrations of the substrate and the reaction product in the diffusion shell, respectively, $D_{S,d}$ and $D_{P,d}$ are the diffusion coefficients of the materials in the bulk solution, R_1 is the radius of the unit cell.

B. Boundary Conditions

Fluxes of the substrate and the product through the stagnant external diffusion shell is assumed to be equal to the corresponding fluxes entering the surface of the microreactor,

$$D_{S,m}\frac{\partial S_m}{\partial r}\Big|_{r=R_0} = D_{S,d}\frac{\partial S_d}{\partial r}\Big|_{r=R_0}, \tag{5a}$$

$$D_{P,m}\frac{\partial P_m}{\partial r}\Big|_{r=R_0} = D_{P,d}\frac{\partial P_d}{\partial r}\Big|_{r=R_0}. \tag{5b}$$

The formal partition coefficient ϕ is used to describe the specificity in concentration distribution of the compounds between two neighboring regions [6][21],

$$S_m(R_0) = \phi S_d(R_0), \quad P_m(R_0) = \phi P_d(R_0). \tag{6}$$

Due to the symmetry of the microreactor, the zero-flux boundary conditions are defined for the center of the microreactor ($r = 0$),

$$D_{S,m}\frac{\partial S_m}{\partial r}\Big|_{r=0} = 0, \quad D_{P,m}\frac{\partial P_m}{\partial r}\Big|_{r=0} = 0. \tag{7}$$

According to the Nernst approach, the shell of thickness $\nu = R_1 - R_0$ remains unchanged with time [15][17]. Away from it, the solution is in motion and is uniform in concentration. Due to the continuous injection of the substrate into the stirred tank and washing off of the product, the concentration in the convective region remains unchanged:

$$S_d(R_1) = S_0, \quad P_d(R_1) = 0. \tag{8}$$

The thickness ν of the Nernst diffusion shell depends upon the nature and stirring up the buffer solution. Usually, more intensive stirring corresponds to the thinner diffusion layer (shell).

 ISBN: 978-1-61208-594-4

C. Microbioreactor Characteristics

In many industrial processes, especially in the production of low-value added products like biopesticides, bio-fertilizers, bio-surfactants ect. [9], it is important to continuously improve the yield and/or productivity [7]. The productivity is important, since this ensures an efficient utilization of the production capacity, i.e., the bioreactors.

The yield of the desired product on the substrate is one of the most important criteria for design and optimization of bioreactors. The economic feasibility of the process is expressed by the yield factor as the ratio of product formation rate and the substrate uptake rate [6][7].

The bioreactor construction is efficient enough when the product emission is relatively large with given substrate amount used. The product emission rate $\bar{E}_{P,O}$ can be calculated by an integration of the product flux over the outer surface of the diffusion shell [7],

$$\begin{aligned}\bar{E}_{P,O} &= \int_0^{2\pi}\int_0^{\pi} D_{P,d}\frac{\partial P_d}{\partial r}\Big|_{r=R_1} R_1^2\sin(\theta)d\theta d\varphi \\ &= 4\pi R_1^2 D_{P,d}\frac{\partial P_d}{\partial r}\Big|_{r=R_1}.\end{aligned} \tag{9}$$

The average consumption $\bar{C}_S$ of the substrate over the whole microreactor can be calculated as follows:

$$\begin{aligned}\bar{C}_S &= \int_0^{R_0}\int_0^{2\pi}\int_0^{\pi}\frac{V_{\max}S_0}{K_M+S_0}\sin(\theta)d\theta d\varphi r^2 dr \\ &= \int_0^{R_0} 4\pi\frac{V_{\max}S_0}{K_M+S_0}r^2 dr \\ &= \frac{4}{3}\pi V_{\max}R_0^3\frac{S_0}{K_M+S_0}.\end{aligned} \tag{10}$$

The yield factor γ for the microreactor system, as well as for the entire tank reactor shown in Figure 1, can be defined by the ratio of the product emission rate to the substrate consumption rate,

$$\gamma = \frac{\bar{E}_{P,O}}{\bar{C}_S}. \tag{11}$$

The yield factor is equal to unity ($\gamma = 1$) when whole the consumed substrate is converted to the product and the whole the product eluted into the bulk (convective region Ω_c). The microbioreactor is absolutely inefficient ($\gamma = 0$), if no product falls into the bulk.

III. Dimensionless model

In order to define the main governing parameters of the two compartment model (3)-(8), the dimensional variable r and unknown concentrations $S_m(r), P_m(r), S_d(r), P_d(r)$ are replaced with the following dimensionless parameters:

$$\begin{aligned}\widetilde{r} = \frac{r}{R_0},\quad \widetilde{S}_m = \frac{S_m}{K_M}, \\ \widetilde{P}_m = \frac{P_m}{K_M},\quad \widetilde{S}_d = \frac{S_d}{K_M},\quad \widetilde{P}_d = \frac{P_d}{K_M},\end{aligned} \tag{12}$$

where $\widetilde{r}$ is the dimensionless distance from the microreactor center and $\widetilde{S}_m(\widetilde{r}), \widetilde{P}_m(\widetilde{r}), \widetilde{S}_d(\widetilde{r}), \widetilde{P}_d(\widetilde{r})$ are the dimensionless concentrations. Having defined dimensionless variables and unknowns, the following dimensionless parameters characterize the domain geometry and the substrate concentration in the bulk:

$$\widetilde{\nu} = \frac{\nu}{R_0},\quad \widetilde{S}_0 = \frac{S_0}{K_M}, \tag{13}$$

where $\widetilde{\nu}$ is the dimensionless thickness of the Nernst diffusion layer (see Figure 2(b)), $\widetilde{S}_0$ is the dimensionless substrate concentration in the bulk solution. The dimensionless thickness of the microreactor equals one.

The governing equations (3) in the dimensionless coordinates are expressed as follows ($0 < \widetilde{r} < 1$):

$$\frac{1}{\widetilde{r}^2}\frac{\partial}{\partial\widetilde{r}}\Big(\widetilde{r}^2\frac{\partial\widetilde{S}_m}{\partial\widetilde{r}}\Big) - \sigma^2\frac{\widetilde{S}_m}{1+\widetilde{S}_m} = 0, \tag{14a}$$

$$\frac{D_{P,m}}{D_{S,m}}\frac{1}{\widetilde{r}^2}\frac{\partial}{\partial\widetilde{r}}\Big(\widetilde{r}^2\frac{\partial\widetilde{P}_m}{\partial\widetilde{r}}\Big) + \sigma^2\frac{\widetilde{S}_m}{1+\widetilde{S}_m} = 0, \tag{14b}$$

where σ is the Thiele modulus or the Damköhler number [7][22][23] defined as:

$$\sigma^2 = \frac{V_{\max}R_0^2}{K_M D_{S,m}}. \tag{15}$$

The governing equations (4) take the following form ($1 < \widetilde{r} < 1+\widetilde{\nu}$):

$$\frac{D_{S,d}}{D_{S,m}}\frac{1}{\widetilde{r}^2}\frac{\partial}{\partial\widetilde{r}}\Big(\widetilde{r}^2\frac{\partial\widetilde{S}_d}{\partial\widetilde{r}}\Big) = 0, \tag{16a}$$

$$\frac{D_{P,d}}{D_{S,m}}\frac{1}{\widetilde{r}^2}\frac{\partial}{\partial\widetilde{r}}\Big(\widetilde{r}^2\frac{\partial\widetilde{P}_d}{\partial\widetilde{r}}\Big) = 0. \tag{16b}$$

The matching conditions (5), (6) and (8) become:

$$\frac{\partial\widetilde{S}_m}{\partial\widetilde{r}}\Big|_{\widetilde{r}=1} = \frac{D_{S,d}}{D_{S,m}}\frac{\partial\widetilde{S}_d}{\partial\widetilde{r}}\Big|_{\widetilde{r}=1} \tag{17a}$$

$$\frac{\partial\widetilde{P}_m}{\partial\widetilde{r}}\Big|_{\widetilde{r}=1} = \frac{D_{P,d}}{D_{S,m}}\frac{\partial\widetilde{P}_d}{\partial\widetilde{r}}\Big|_{\widetilde{r}=1}. \tag{17b}$$

$$\widetilde{S}_m(1) = \phi\widetilde{S}_d(1),\quad \widetilde{P}_m(1) = \phi\widetilde{P}_d(1). \tag{18}$$

$$\frac{\partial\widetilde{S}_m}{\partial\widetilde{r}}\Big|_{\widetilde{r}=0} = 0,\quad \frac{\partial\widetilde{P}_m}{\partial\widetilde{r}}\Big|_{\widetilde{r}=0} = 0, \tag{19a}$$

$$\widetilde{S}_d(1+\widetilde{\nu}) = \widetilde{S}_0,\quad \widetilde{P}_d(1+\widetilde{\nu}) = 0. \tag{19b}$$

The dimensionless factor σ^2 essentially compares the rate of enzyme reaction ($V_{\max}/K_M$) with the diffusion through the enzyme-loaded microreactor ($D_{S,m}/R_0^2$). If $\sigma^2 \ll 1$, the enzyme kinetics controls the bioreactor action. The action is under diffusion control when $\sigma^2 \gg 1$.

The Biot number β is another dimensionless parameter widely used to indicate the internal mass transfer resistance to the external one [24][25],

$$\beta = \frac{D_{S,d}R_0}{D_{S,m}(R_1 - R_0)}. \tag{20}$$

 ISBN: 978-1-61208-594-4

When the Biot number is small, the effect of the external diffusion is the most marked. As the Biot number increases the effect of the external diffusion becomes less important.

The diffusion module and the Biot number are widely used in analysis and design of different bioreactors [25]. The experiment conducted by Kont et al. [10] proved the external mass-transfer limitations to be negligible for $\beta > 1$ using the first order kinetics model of CSTR and packed-bed reactors (PBR), which conducted condition (8). Typically, designers seek for bioreactors acting in the reaction-limited regime, since in this case reaction and diffusion occur on different time scales [26].

IV. Digital simulation of experiments

The non-linearity of the governing equations prevents us from solving the boundary value problem (14)-(19) analytically, hence the numerical model was constructed and solved using finite difference technique [17]. An explicit scheme was used; however since Michaelis-Menten non-linearity, further construction of equations was used:

$$D_{C,m} \cdot \frac{1}{r^2}\frac{\partial}{\partial r}\left(r^2 \frac{\partial C_m^n}{\partial r}\right) = \pm \frac{V_{\max} C_m^n}{K_M + C_m^{n-1}},$$

where $C = S, P$. Tridiagonal matrix was constructed from the equations. In the numerical simulation, scheme was run until the following loss becomes very small:

$$\mathcal{L} = ||S^n - S^{n-1}||_{l^2} + ||P^n - P^{n-1}||_{l^2} < \epsilon,$$

where decay rate value $\epsilon = 10^{-14}$ was used over l^2 norm. An explicit finite difference the scheme was built on a uniform discrete grid with 128 points in space direction [16]. The simulator has been programmed by the authors in C++ language [27].

The numerical solution of the mathematical model (14)-(19) was validated by using exact analytical solutions known for very special cases of the model parameters [22][25][6][16]. At such low concentration of the substrate as $S_0 \ll K_M$, the non-linear reaction rate in equations (3) reduces to the first order reaction rate. In very opposite case, when the substrate concentration S_0 to be measured is very high compared to the Michaelis constant K_M ($S_0 \gg K_M$), the reaction term reduces to the zero order reaction rate $V_{\max}$.

V. Results and discussion

To investigate the effects of the geometry and catalytic activity of the microreactor, the reactor action was simulated and the yield factor was calculated for very different values of the Biot number β, the Thiele module σ and the substrate dimensionless concentration S_0.

A. Concentration profiles

Figure 3 shows the profiles of the product concentration P calculated from the microreactor model (14)-(19) changing the Thiele module σ as well as the Biot number β, and keeping unchanged the following model parameters:

$$D_{S,m} = D_{P,m}, \quad D_{S,d} = D_{P,d}, \quad \phi = 0.5, \quad \widetilde{\nu} = 1. \qquad (21)$$

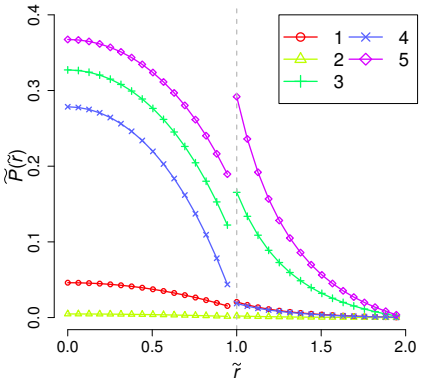

Figure 3. Concentration profiles of the product in the microreactor simulated at the substrate concentration $\widetilde{S}_0 = 1$ and different values of the Thiele module σ^2: 0.1 (2), 1 (1), 10 (3-5), as well as the Biot number β: 0.5 (5), 1 (1-3), 10 (4), the other parameters are as defined in (21). Dashed line shows boundary between the microreactor and the diffusion layer.

One can be seen in Figure 3, that low Thiele modulus values $\sigma < 1$ or high Biot number values, which means that the species passes the Nernst diffusion layer fast, give the concentrations approach to straight line because of linearity of governing equations in the area $r \in (1, 1 + \widetilde{\nu})$. On the other hand, high Thiele modulus values ($\sigma^2 \geq 10$) lead to significant differences in concentration distribution across the outer boundary of the microreactor.

B. Impact of the substrate concentration

To investigate the dependence of the yield factor γ on the substrate concentration $\widetilde{S}_0$, γ was calculated by simulating the microreactor action at three characteristic values of the Thiele module σ^2: 0.1, 1 and 10, as well as at three values of the Biot number β: 0.5, 1 and 10. The effect of the substrate concentration was investigated in a wide range of $\widetilde{S}_0$ values $[10^{-3}, 10^3]$. Calculation results are presented in Figure 4.

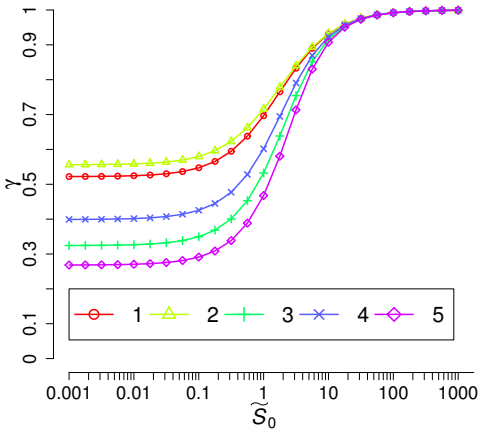

Figure 4. The yield factor γ vs. the substrate concentration $\widetilde{S}$. The notation and values of the parameters are the same as in Figure 3.

One can see (Figure 4) a non-linear impact of the substrate concentration on the yield factor.

As a function of $\widetilde{S}_0$, the yield factor γ is a monotonous increasing function with limit of one. At low concentrations of

the substrate $\widetilde{S_0} < 1$, the yield factor increases with decreasing the Thiele modulus and increasing the Biot number β.

The yield factor γ is, practically, invariant to changes in the substrate concentration $\widetilde{S_0}$ when the Michaelis-Menten kinetics approaches the first order ($\widetilde{S_0} \ll 1$) or zero order kinetics ($\widetilde{S_0} \gg 1$). At intermediate values of $\widetilde{S_0}$, when the kinetics changes from the first to zero order, the yield factor γ noticeably increases with increasing the substrate concentration. Increasing the substrance concentration does not influence the increase in the product yield for $\widetilde{S_0} > 100$.

C. Impact on product rate

Figure 5 presents the dependence of the product emission rate on the thickness of the Nernst diffusion layer. Values of $\bar{V}_{P,0}$ were calculated changing the dimensionless thickness $\widetilde{\nu}$ of the Nernst diffusion layer from $10^{-0.5}$ up to $10^{0.75}$. At lower values of $\widetilde{\nu}$ the two compartment model (14)-(19) reduces to a notably simpler one layer model [22][25]. The reactor behaviour at larger values of $\widetilde{\nu}$ is not so important due to the product emission at very low rate.

As one can see in Figure 5, the rate $\bar{V}_{P,0}$ is a decreasing function of $\widetilde{\nu}$, which confirms a hypothesis about the importance of the Nernst layer for the reactors productivity [25]. The decrease in $\bar{V}_{P,0}$ with increasing $\widetilde{\nu}$ is especially noticeable at relatively high substrate concentrations ($\widetilde{S_0} = 10$, curve 4), as well as high values of the Thiele module ($\sigma^2 = 2$, curve 2), i.e. in the case of the first order kinetics or when the reactor is under the diffusion control.

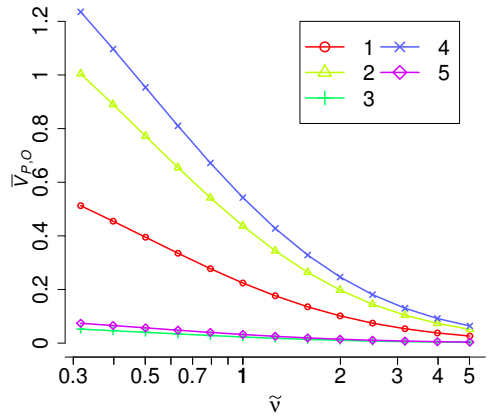

Figure 5. The product emission rate $\bar{V}_{P,0}$ vs. the dimensionless thickness $\widetilde{\nu}$ of the Nernst diffusion layer at $\widetilde{S_0}$: 0.1 (5), 1 (1-3), 10 (4), σ^2: 0.1 (3), 1 (1, 4, 5), 2 (2), the other parameters are as defined in (21).

The impact of the thickness $\widehat{\nu}$ on the product rate $\bar{V}_{P,0}$ gives us tendencies on thickness $\widehat{\nu}$ selection. However, reducing the thickness of Nernst layer is a serious problem. Since microreactor is soaking and mixing to create layer and zero thickness of the diffusion shell can not be achieved [15], the impact of other model parameters on the microreactor efficiency is also important.

D. Impact of the Biot number

To investigate the dependence of the yield factor γ on the Biot number β, the factor γ was calculated at different values of the Thiele module σ^2 (0.1, 1 and 10) and the substrate concentration $\widetilde{S_0}$ (0.1, 1 and 10), changing the Biot number in a range of $[10^{-1}, 10^2]$. The results of the calculations are depicted in Figure 6.

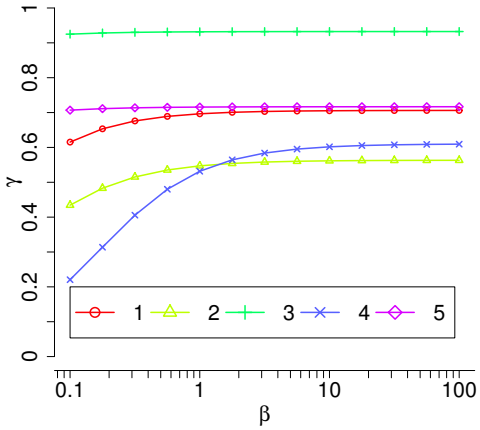

Figure 6. The yield factor γ vs. the Biot number β at $\widetilde{S_0}$: 0.1 (2), 1 (1, 4, 5), 10 (3), σ^2: 0.1 (5), 1 (1-3), 10 (4), the other parameters are as in (21).

Figure 6 shows the product yield γ as an increasing function of the Biot number β. However, the yield factor γ rapidly grows only when β values are relatively small ($\beta < 1$), and the reactor action is under the diffusion control ($\sigma > 1$). The yield factor, practically, does not depend on β when the microreactor acts under the enzyme kinetics control ($\sigma < 1$) or the substrate concentration is high ($\widetilde{S_0} > 10$). On the other hand, the Nernst diffusion layer may be neglected when the Biot number is higher than around 20 [25][28].

E. Impact of the Thiele Module

The dependence of the yield factor γ on the Thiele modulus was investigated by calculating the factor γ at different values of the Biot number β, as well as of the substrate concentration $\widetilde{S_0}$ and changing modulus σ from 10^{-3} up to 10^5. Figure 6 shows the yield factor γ as a monotonous decreasing function of σ at very different values of β and $\widetilde{S_0}$.

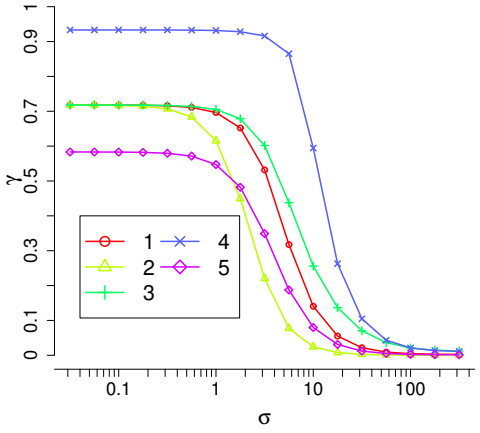

Figure 7. The yield factor γ vs. the Thiele modulus σ at β: 0.1(2), 1(1, 4, 5), 10(3), $\widehat{S_0}$: 0.1(5), 1(1-3), 10(4), the other parameters are as in (21).

 ISBN: 978-1-61208-594-4

It can be seen in Figure 7 that the yield factor γ, practically, does not depend on σ and approaches to zero when the bioreactor acts notably under the diffusion control ($\sigma > 100$). The yield factor γ is also invariant to changes in the modulus σ when the enzyme kinetics controls the bioreactor action ($\sigma < 0.01$). At mixed conditions when the reactor action is influenced by both the enzyme kinetics and the diffusion, the yield factor γ noticeably decreases with increasing the modulus σ. Figure 7 also shows that the factor γ increases with increasing the substrate concentration (as in Figure 4), as well as when increasing the Biot number β (as in Figure 6).

There are some limitations worth to mention that might be used for the future investigations. First of all, in physical experiments, pellets will not be perfect spheres, which requires modelling more sophisticated domains in 2D and 3D space. Secondly, the system with time dependent characteristics should be considered in the future work.

VI. Conclusion and Future Work

The mathematical model (3)-(8) of the microbioreactor can be successfully used to investigate the behaviour of the catalytic microreactor and to optimize its configuration.

The thickness of the Nernst diffusion layer (shell) noticeably effects the reaction product emission (Figures 5, 6). The production rate $\bar{V}_{P,0}$ as well as the yield especially decreases when the thickness is more than two times greater than the radius of the microreactor, $\widetilde{\nu} > 2$, $\beta < 0.5$. This property becomes important when the size of microbioreactors used in industrial applications continuously reduces, while the Nernst diffusion layer is still often neglected.

The yield of the product increases with increasing the substrate concentration (Figure 4) and with decreasing the Biot number (Figure 6). However, an increase in the substrate concentration becomes ineffective when the enzyme reaction apporaches the zero order kinetics $\widetilde{S}_0 > 10$ (Figure 4). The high yield can be achieved only when the enzyme kinetics controls the bioreactor action $\sigma < 1$ (Figure 7).

Such formulation can be useful to find optimal parameters of such biosystem construction [11]. More importantly, it might improve the design and production of microbioreactors.

More precise and sophisticated computational models, implying the multiple reactions of microreactor, as well as the observed experimental data of the microreactors for model validation are still under development.

References

[1] A. Regalado-Mndez, R. R. Romero, R. N. Rangel, and S. Skogestad, "Biodiesel Production in Stirred Tank Chemical Reactors: A Numerical Simulation," in *New Trends in Networking, Computing, E-learning, Systems Sciences, and Engineering*. Springer, 2015, pp. 109–116.

[2] O. N. Ada and D. T. Sponza, "Anaerobic/aerobic treatment of municipal landfill leachate in sequential two-stage up-flow anaerobic sludge blanket reactor (UASB)/completely stirred tank reactor (CSTR) systems," *Process Biochemistry*, vol. 40, no. 2, pp. 895–902, 2005.

[3] A. Miyawaki, S. Taira, and F. Shiraishi, "Performance of continuous stirred-tank reactors connected in series as a photocatalytic reactor system," *Chemical Engineering Journal*, vol. 286, pp. 594–601, 2016.

[4] M. A. Dareioti and M. Kornaros, "Effect of hydraulic retention time (HRT) on the anaerobic co-digestion of agro-industrial wastes in a two-stage CSTR system," *Bioresource Technology*, vol. 167, pp. 407–415, 2014.

[5] A. J. Straathof and P. Adlercreutz, *Applied Biocatalysis*. CRC Press, 2000.

[6] P. M. Doran, *Bioprocess Engineering Principles*. Academic Press, 1995.

[7] J. Villadsen, J. Nielsen, and G. Liden, *Bioreaction Engineering Principles*. Dordrecht: Springer, 2011.

[8] S. K. Dubey, A. Pandey, and R. S. Sangwan, *Current Developments in Biotechnology and Bioengineering: Crop Modification, Nutrition, and Food Production*. Elsevier, 2016.

[9] J. W. Wong, R. D. Tyagi, and A. Pandey, *Current Developments in Biotechnology and Bioengineering: Solid Waste Management*. Elsevier, 2016.

[10] A. Konti, D. Mamma, D. G. Hatzinikolaou, and D. Kekos, "3-Chloro-1, 2-propanediol biodegradation by Ca-alginate immobilized Pseudomonas putida DSM 437 cells applying different processes: mass transfer effects," *Bioprocess and Biosystems Engineering*, vol. 39, no. 10, pp. 1597–1609, 2016.

[11] D. Cacaval, A. C. Blaga, and A.-I. Galaction, "Diffusional effects on anaerobic biodegradation of pyridine in a stationary basket bioreactor with immobilized Bacillus spp. cells," *Environmental Technology*, pp. 1–13, 2017.

[12] R. Karande, A. Schmid, and K. Buehler, "Applications of multiphasic microreactors for biocatalytic reactions," *Organic Process Research & Development*, vol. 20, no. 2, pp. 361–370, 2016.

[13] F. M. Pereira and S. C. Oliveira, "Occurrence of dead core in catalytic particles containing immobilized enzymes: analysis for the michaelis–menten kinetics and assessment of numerical methods," *Bioprocess and Biosystems Engineering*, vol. 39, no. 11, pp. 1717–1727, 2016.

[14] M. B. Kerby, R. S. Legge, and A. Tripathi, "Measurements of kinetic parameters in a microfluidic reactor," *Analytical Chemistry*, vol. 78, no. 24, pp. 8273–8280, 2006.

[15] J. Wang, *Analytical Electrochemistry*, 3rd ed. Joboken, New Jersey: John Wiley & Sons, 2006.

[16] R. Baronas, F. Ivanauskas, and J. Kulys, *Mathematical Modeling of Biosensors*. Dordrecht: Springer, 2010.

[17] D. Britz and J. Strutwolf, *Digital Simulation in Electrochemistry*, 4th ed., ser. Monographs in Electrochemistry. Springer, 2016.

[18] M. F. Chaplin and C. Bucke, "The large-scale use of enzymes in solution," *Enzyme Technology*, pp. 138–166, 1990.

[19] H. Gutfreund, *Kinetics for the Life Sciences*. Cambridge: Cambridge University Press, 1995.

[20] L. A. Segel and M. Slemrod, "The quasi-steady-state assumption: a case study in perturbation," *SIAM Review*, vol. 31, no. 3, pp. 446–477, 1989.

[21] M. Velkovsky, R. Snider, D. E. Cliffel, and J. P. Wikswo, "Modeling the measurements of cellular fluxes in microbioreactor devices using thin enzyme electrodes," *Journal of Mathematical Chemistry*, vol. 49, no. 1, pp. 251–275, 2011.

[22] T. Schulmeister, "Mathematical modelling of the dynamic behaviour of amperometric enzyme electrodes," *Selective Electrode Reviews*, vol. 12, no. 2, pp. 203–260, 1990.

[23] D. J. Fink, T. Na, and J. S. Schultz, "Effectiveness factor calculations for immobilized enzyme catalysts," *Biotechnology and Bioengineering*, vol. 15, no. 5, pp. 879–888, 1973.

[24] R. Aris, *Mathematical Modeling: a Chemical Engineer's Perspective*. Academic Press, 1999, vol. 1.

[25] M. E. Davis and R. J. Davis, *Fundamentals of Chemical Reaction Engineering*. New York: MGraw-Hill, 2003.

[26] D. A. Edwards, B. Goldstein, and D. S. Cohen, "Transport effects on surface-volume biological reactions," *Journal of Mathematical Biology*, vol. 39, no. 6, pp. 533–561, 1999.

[27] W. T. Vetterling, *Numerical Recipes Example Book (C++): The Art of Scientific Computing*. Cambridge University Press, 2002.

[28] R. Baronas, "Nonlinear effects of diffusion limitations on the response andsensitivity of amperometric biosensors," *Electrochimica Acta*, vol. 240, pp. 399–407, 2016.

 ISBN: 978-1-61208-594-4